

Comparison of the $^{27}\text{Al}(^3\text{He}, ^3\text{He}')^{27}\text{Al}$ and $^{27}\text{Al}(^3\text{He}, t)^{27}\text{Si}$ Reactions at 18 MeV*

J. E. Holden,† D. P. Balamuth, H. T. Fortune, and R. W. Zurmühle
Physics Department, University of Pennsylvania, Philadelphia, Pennsylvania 19104
 (Received 25 July 1972)

The $^{27}\text{Al}(^3\text{He}, ^3\text{He}')^{27}\text{Al}$ and $^{27}\text{Al}(^3\text{He}, t)^{27}\text{Si}$ reactions have been studied at an incident-beam energy of 18 MeV. Angular distributions were measured for many low-lying states. The transitions to states below 3.00 MeV excitation in the two reactions were compared using the macroscopic-interaction model of the distorted-wave Born approximation, using a generalized isospin-dependent optical-model potential. The observed $L=4$ strength in the $(^3\text{He}, t)$ reaction is inconsistent with both the inelastic scattering results of this work and other measurements of the hexadecapole deformation in this region, indicating that the inelastic scattering and charge-exchange processes may be microscopically more distinct than is suggested by the macroscopic model. Angular distributions for states in ^{27}Si above 3 MeV excitation are also presented and discussed. The $(^3\text{He}, t)$ study also showed that the ^{27}Si state of $E_x=4.46$ MeV is an unresolved doublet, confirming other recent work.

I. INTRODUCTION

The formal similarity of the charge-exchange and inelastic scattering processes has long been recognized. In particular, many methods of interpretation and analysis originally developed for inelastic scattering have been successfully applied to charge-exchange reactions; these include the method of coupled channels,¹ the distorted-wave Born approximation (DWBA) using both microscopic² and macroscopic^{3,4} models of the effective interaction, and the diffraction model.⁵

The microscopic distorted-wave model of inelastic scattering and charge exchange requires detailed knowledge of the shell-model structure of the initial and final nuclear states. The nuclei ^{27}Si and ^{27}Al are believed to be somewhat deformed, although the description of the mass-27 system has been quite controversial. In view of the uncertainties concerning the microscopic description of the nuclei ^{27}Si and ^{27}Al , in the present work the analysis has been performed using the collective or macroscopic model.

In the collective distorted-wave model of inelastic scattering the projectile-target interaction is expressed as a nonspherical optical potential. The deformed shape of this interaction potential is taken to be identical with that of the mass distribution in the target nucleus. The interaction excites target-collective excitations of angular momentum L with an amplitude directly proportional to β_L , the deformation amplitude of multipole order L .⁶

Thus measurements of inelastic scattering cross sections can yield (reaction model-dependent) values of these deformations. The proportionality holds whether β_L represents permanent

deviations from sphericity in the body-fixed system (rotational excitations) or the average value of dynamic deviations from sphericity in the space-fixed system (vibrational excitations).

It should be noted that this reaction model allows only direct one-step processes regardless of multipole order L . In some cases, however, specific inelastic channels are strongly coupled to the entrance channel. These can often be treated using the coupled-channels formalism⁷ where the scattering wave functions in a limited number of inelastic reaction channels are computed together, taking into account the couplings among these channels. Again, values of β_L can be extracted from the calculations; these are in general different from those derived from the DWBA calculations. If, however, the couplings between a given channel and the remaining channels are all weak, and all excited-state channels have amplitudes small compared to the elastic scattering channel, the two reaction models yield quite similar results. The deviations from sphericity β_L can also be measured by means of electromagnetic interactions; comparison of these values with those derived from inelastic scattering can thus provide a measure of the validity of the model used.

The DWBA inelastic scattering formalism can be applied to charge-exchange reactions by including an isospin-dependent term in the generalized optical-model potential⁸

$$U(\vec{r}) = U_0(\vec{r}) + \frac{1}{A} U_1(\vec{r}) \vec{t} \cdot \vec{T}_0, \quad (1)$$

where \vec{t} and \vec{T}_0 are the projectile and target isospin vectors, respectively, A is the target mass number, and $U_0(\vec{r})$ and $U_1(\vec{r})$ are in general dif-

ferent functions of the vector displacement \vec{r} between the projectile and target centers of mass. Charge-exchange reactions proceed by virtue of the off-diagonal matrix elements of the operator $\vec{t} \cdot \vec{T}_0$ in isospin space. Charge-exchange transitions to the isobaric analog of the target ground states (analog transitions) have been successfully treated in the DWBA using the second term in Eq. (1) as a perturbation on elastic scattering,^{3, 4} and in the coupled-channels formalism, coupling the analog transition to the elastic scattering channel by means of the interaction (1).¹ Nonanalog transitions can be accommodated by allowing the interaction potential $U_1(\vec{r})$ to be deformed.

It is these nonanalog charge-exchange transitions that are of primary interest in the present study. Previous collective-model studies^{3, 4} of nonanalog charge-exchange transitions have been carried out principally for even- A targets in the $1f_{7/2}$ shell. The results of these studies have been summarized and discussed by Satchler.⁸ The strength of the interaction U_1 is yielded by fitting the analog-transition data, using a complex surface-peaked interaction. The part of the interaction with the larger radius, usually taken as the imaginary part, dominates the interaction and is responsible for essentially all the charge-exchange cross section. If this interaction is then used to calculate nonanalog quadrupole transitions in the DWBA using the first-order collective model, the experimental angular-distribution shapes are well reproduced. The question of agreement between theoretical and experimental magnitudes of the cross sections is somewhat less clear. The strengths U_1 of Eq. (1) yielded by analog transitions are known to be very sensitive to the geometry of the effective interaction³ and to the incident-projectile energy.⁹ In addition, the deformation amplitudes β yielded by the nonanalog transitions are not in general equal to those measured in inelastic scattering, and are sometimes found to be even two or three times larger.⁴ Kunz *et al.*⁴ point out that the nonanalog transitions are sensitive to the neutron-excess deformation only, which can in general be quite different from that of the whole nucleus. Finally, it should be noted that higher-order processes may influence this measurement of the neutron-excess deformation. The isoscalar part of the potential $U(\vec{r})$ can effect inelastic scattering either before or after a charge-exchange analog transition, reaching the same final state as the one-step nonanalog transition. Frahn⁵ has shown that these two-step processes are expected to be of comparable strength as the one-step process. Thus they could account for large experimental values of β . Population of the final state by compound-nuclear

processes would of course have similar effects.

The situation is here further investigated by the study and comparison of the $^{27}\text{Al}(^3\text{He}, ^3\text{He}')^{27}\text{Al}$ and the $^{27}\text{Al}(^3\text{He}, t)^{27}\text{Si}$ reactions at an incident energy of 18 MeV. The assumption that the low-lying states of ^{27}Al and ^{27}Si have large parentage in the low-lying collective excitations of ^{28}Si provides an interpretation of the inelastic scattering and charge-exchange reactions in terms of the collective-model DWBA. This interpretation is described in detail in Sec. III.

II. EXPERIMENTAL PROCEDURE AND RESULTS

The $^{27}\text{Al}(^3\text{He}, ^3\text{He}')^{27}\text{Al}$ and $^{27}\text{Al}(^3\text{He}, t)^{27}\text{Si}$ reactions were studied using a beam of 18-MeV $^3\text{He}^{++}$ ions from the University of Pennsylvania tandem accelerator. Self-supporting aluminum foils of $70\text{-}\mu\text{g}/\text{cm}^2$ thickness were placed in the center of a 61-cm-diam scattering chamber. Emerging particles were detected in a system of silicon surface-barrier detector telescopes; ΔE and E detector thicknesses were $100\ \mu\text{m}$ and $2\ \text{mm}$, respectively. Energy signals were digitized and processed in a ND-3300/PDP-9 analyzer-computer system. Digital particle identification was performed on line using the range-energy relationship of charged particles in silicon as suggested by Goulding *et al.*¹⁰

For each event the quantity $P = (E + \Delta E)^{1.76} - E^{1.76}$ was computed, where ΔE is the energy loss in the front detector, and E is the energy loss in the rear detector. This quantity has a characteristic value for each particle type. The required exponentiation was performed using a table lookup technique. During the acquisition of the data all events having values of P corresponding to tritons or ^3He were written onto magnetic tape. The requirement was set to ensure that no triton or ^3He events were missed; some deuteron or α events were consequently stored as well. After the experiment the magnetic tapes were analyzed using the same PDP-9 computer. In this final data reduction the value of P was set to accept either all triton or all ^3He events. Separate spectra for each reaction were thus obtained at each angle.

The spectra at different angles were normalized using the number of elastic scattering events recorded in a monitor detector. Absolute cross sections were obtained by assuming that the elastic scattering cross section of ^3He on ^{27}Al at forward angles is correctly given by the optical model, with the parameters given in Table I. The relative solid angles of the counter telescopes and the monitor detector were measured using an ^{241}Am α source. The uncertainty assigned to the absolute cross-section measurements is $\pm 30\%$.

Typical triton and ^3He energy spectra are shown in Fig. 1. The ^{27}Al elastic scattering peak is absent from the ^3He spectrum because elastic events were rejected during data accumulation using a single-channel analyzer which set an upper limit on the total particle energy. The calculated mean centroid of the unresolved 2.98–3.00-MeV doublet in the inelastic scattering data is 3.00 MeV and thus this peak is taken to be dominated by the 3.00-MeV $J^\pi = \frac{9}{2}^+$ level. Figure 2 shows triton spectra at three angles for the region of excitation near 4.40 MeV. The fact that the peak labeled 4.46 MeV is consistently wider than that of the nearby 4.30-MeV level is indicative of the presence of a new state in ^{27}Si very near the previously known state at 4.46 MeV. This observation substantiates that of Barker *et al.*,¹¹ who recently reported exciting both members of the doublet in the $(^3\text{He}, \alpha)$ reaction.

Angular distributions for thirteen levels in ^{27}Si were measured in 5° steps from 10 to 75° laboratory angle. Angular distributions for five levels in ^{27}Al were measured in 5° steps from 20 to 75° laboratory angle. The levels above 3.0 MeV in ^{27}Al were excited only weakly relative to the low-lying states.

III. METHODS OF ANALYSIS

A. Distorted-Wave Theory of Inelastic Scattering

The collective-model distorted-wave theory of inelastic scattering has been described by Bassel *et al.*,⁶ and will be only summarized here. The projectile-target interaction is expressed in terms of a nonspherical optical potential $U(r-R)$. The deformed shape of this potential is taken to be identical to that of the target-mass distribution, expressed by the following multipole expansion of the nuclear radius:

$$R(\Theta, \varphi) = R_0 + \delta R(\Theta, \varphi) = R_0 + R_0 \sum_{lm} \alpha_{lm} Y_{lm}(\Theta, \varphi). \quad (2)$$

The optical potential is expanded in a Taylor series in powers of the displacement $\delta R(\Theta, \varphi)$; the usual DWBA formalism then yields for the transition amplitude for the excitation of a state J by

angular momentum transfer l :

$$T_{if}^l = (2l+1)^{1/2} i^l I_{lm} \langle J_i M_i l m | J_f M_f \rangle \times \frac{R_0 U \beta_l}{(2l+1)^{1/2} (2S_0+1)^{1/2}}, \quad (3)$$

where

$$(2l+1)^{1/2} i^l I_{lm} = \int \chi^{(-)*}(\vec{k}_f, \vec{r}) F(r-R_0) \times Y_l^m(\vec{r}) \chi^{(+)}(\vec{k}_i, \vec{r}) d^3r. \quad (4)$$

$\chi^{(-)}(\vec{k}_f, \vec{r})$ and $\chi^{(+)}(\vec{k}_i, \vec{r})$ are distorted waves appropriate to the exit and entrance channels, respectively. S_0 is the intrinsic spin of the projectile; it has been assumed that the distorted waves have been calculated without spin-dependent forces. The quantity β_l is the deformation amplitude described in the Introduction, and is related to the quantities α_{lm} of Eq. (2). The physical interpretations of β_l in the various collective structural models are presented in Ref. 6. The strength U and the radial function $F(r-R_0)$ in Eqs. (3) and (4) represent the strength and radial dependence of the part of the total optical-model interaction appropriate to the transition. For quadrupole inelastic scattering, they conventionally correspond to the first derivative of the real part of the optical-model potential.⁶ Although there is increasing evidence that the interaction for quadrupole inelastic scattering of ^3He may include an imaginary part,¹² inelastic scattering at the energy and angular range of this study is not very sensitive to this distinction.

Reference 6 includes a discussion of the limits of validity of this model; limits based on multistep processes have already been discussed in the Introduction. The validity of the use of the DWBA is based, of course, on the strength of the inelastic transitions relative to elastic scattering. For quadrupole inelastic scattering, β_2 values up to about 0.25 are usually assumed to imply a sufficiently weak process to warrant use of the DWBA.⁶

B. Extension to Charge-Exchange Transitions

If the optical potential $U(r-R)$ is generalized to include an isospin-dependent term⁸

TABLE I. ^3He and t optical-model parameters for $A=27$.

| V (MeV) | r_v (fm) | a_v (fm) | V_{so} (MeV) | W (MeV) | r_w (fm) | a_w (fm) | V_{soi} (MeV) | r_c (fm) |
|--------------|---------------|---------------|--------------------------|--------------|---------------|---------------|---------------------------|---------------|
| 177 | 1.14 | 0.724 | 0.0 | 21.1 | 1.602 | 0.77 | 0.0 | 1.4 |

$$U(r-R, r-R') = U_0(r-R) + \frac{U_1(r-R')}{A} \vec{t} \cdot \vec{T}_0 \quad (5)$$

then the distorted-wave theory of inelastic scattering can be extended to include charge-exchange transitions. The quantities \vec{t} and \vec{T}_0 are the projectile and target isospin vectors, respectively, and A is the target mass number. The use of the function $R'(\Theta, \varphi)$ permits the deformation of the isospin-dependent term to be different in general from that of the isospin-independent term.

Charge-exchange transitions arise from the off-diagonal matrix elements of the isospin-dependent term in isospin space. For the case of ${}^3\text{He}$ incident on an ${}^{27}\text{Al}$ target, the relevant matrix element is

$$\begin{aligned} \langle T_0 = \frac{1}{2} T_{03} = -\frac{1}{2} t_3 = \frac{1}{2} | \vec{t} \cdot \vec{T}_0 | T_0 = \frac{1}{2} T_{03} = \frac{1}{2} t_3 = -\frac{1}{2} \rangle \\ = -\frac{1}{2} (N-Z)^{1/2} = -\frac{1}{2}, \end{aligned} \quad (6)$$

where N and Z are the target neutrons and proton numbers, respectively. The spherical part of $[U_1(r-R')/A] \vec{t} \cdot \vec{T}_0$ thus effects direct single-step transitions to the isobaric analog of the target ground state. In exact correspondence to the col-

lective model of inelastic scattering, the deformed part of this same interaction causes direct single-step transitions to the analogs of the target collective excitations.

For the analog transition the product $UF(r-R_0)$ of Eqs. (3) and (4) is taken to be complex and surface peaked; the geometric parameters of the real and imaginary parts are conventionally set equal to those of the optical-model potential.^{3,4} The interaction for nonanalog transitions is the derivative of this interaction. The strengths and radial form factors used in all calculations are listed in Table II.

C. Odd- A Targets in the Weak-Coupling Model

The weak coupling of a single-particle state of angular momentum j to a collective excitation of angular momentum L results in a multiplet of levels of angular momentum J_f where $|L-j| \leq J_f \leq L+j$. The DWBA formalism of Sec. IIIA can be extended to include the inelastic excitation of this multiplet. The interaction $U(\vec{r})$ does not depend explicitly on the single-particle coordinates of the weakly coupled particle; thus the presence of the weakly coupled particle enters into the formalism only through angular momentum coupling and spin statistical factors. If the even- A collective ex-

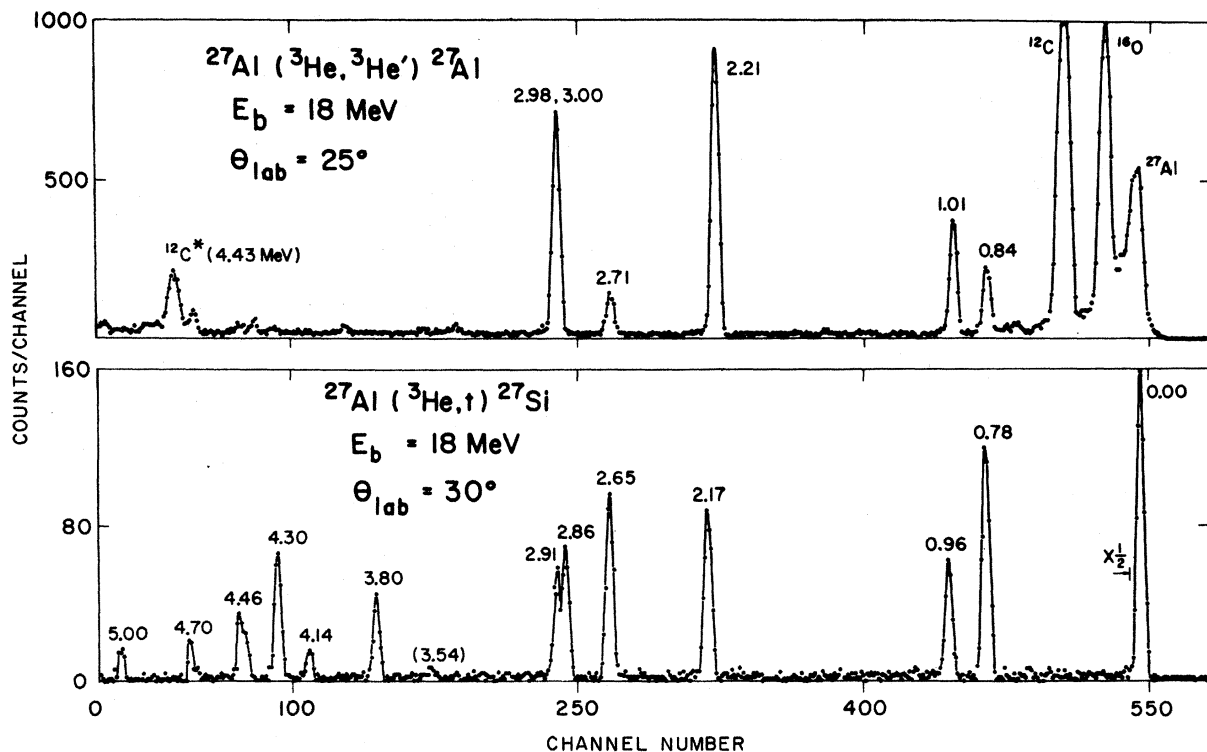


FIG. 1. Representative energy spectra from the ${}^{27}\text{Al}({}^3\text{He}, {}^3\text{He}'){}^{27}\text{Al}$ and ${}^{27}\text{Al}({}^3\text{He}, t){}^{27}\text{Si}$ reactions. Energy levels are labeled in MeV.

citation is excited with the cross section σ_L , then the states of spin J_f share this excitation strength according to

$$\left(\frac{d\sigma}{d\Omega}\right)_{LJ_f} = \frac{2J_f + 1}{(2j + 1)(2L + 1)} \sigma_L. \quad (7)$$

The sum over J_f of these cross sections is equal to σ_L . Thus the validity of the weak coupling picture can be tested by comparing the sum of the cross sections for the odd- A multiplet with that of the even- A collective excitation.

D. Calculations

The optical-model parameters used in all calculations are shown in Table I. These values were used unchanged for both the ^3He and t scattering channels. The calculations were carried out using the DWBA code DWUCK¹³; the collective-model option was employed. For all inelastic scattering calculations the form factor was specified as the derivative of the real part of the entrance-channel optical potential. This corresponds to a surface-peaked interaction with the parameters shown in Table II. For the charge-exchange analog transition, a complex surface-peaked form was assumed for the interaction $U_1(\vec{r})$. The geometric parameters of the real and imaginary parts were those of the real and imaginary parts of the optical potential. The strength U_1 was determined by visually normalizing the calculation to the data. The interaction used for transitions to the excited states was the derivative of the interaction $U_1(\vec{r})$, using the magnitude fixed by the analog transition. The various interactions used are summarized in Table II. Fits to the data were made visually; in the cases of L mixture, the mixtures were ob-

tained by a least-squares-fitting procedure.

The entire procedure was checked for consistency with the existing literature by fitting the data presented in Refs. 3 and 4 with our procedure, and comparing the results with those obtained in these references. We fitted the $(^3\text{He}, t)$ transitions to the analog of the target ground states, using the optical potentials given; a visual fit to the data of Refs. 3 and 4 yielded values for the transition strength U_1 in agreement with those found by those authors. With these values of U_1 the transitions presented in Refs. 3 and 4 to the excited 2^+ states were fitted; the deformations obtained agreed with the original results. We were thus assured that we are using the same prescription as given in Refs. 3 and 4.

The sensitivity of the $(^3\text{He}, t)$ calculations to changes in optical-model parameters was investigated by varying the distorting potentials but keeping the form factor fixed. Calculations were performed for two parameter sets other than those of Set 1, listed in Table I. These were Set 2: $V = 130$ MeV, $W = 21.1$ MeV, $r_v = 1.31$ fm, $r_w = 1.602$ fm, $a_v = 0.724$ fm, and $a_w = 0.770$ fm, and Set 3: $V = 155$ MeV, $W = 20.1$ MeV, $r_v = 1.14$ fm, $r_w = 1.60$ fm, $a_v = 0.75$ fm, and $a_w = 0.71$ fm. Potential Set 2 is related to Set 1 through the Vr_v^2 ambiguity. Set 3 has previously been used in a description of the $^{29}\text{Si}(^3\text{He}, t)^{29}\text{P}$ reaction.¹⁴ All three potential sets give similar predictions for ^3He elastic scattering. The shapes of the calculated angular distributions in the first 60° are virtually identical for the three different potentials, for all L values. However, the predicted magnitudes of the cross section do depend on the potential. For the analog $^{27}\text{Al}(^3\text{He}, t)^{27}\text{Si}$ (g.s.) transition, the predicted cross section at 0° is 20% larger for potential 3 than for potential 1. For Set 2, the 0° cross section is 30% smaller than that calculated with Set 1. Thus, since the cross section is proportional to U_1^2 , these results indicate that uncertainties in the distorting potentials may lead to uncertainties of $\pm 15\%$ in the extracted values of U_1 . This uncertainty is small compared with uncertainties arising from other effects, e.g., incomplete knowledge of the form factor. The deformation parameters β extracted from the nonanalog transitions are even less sensitive to changes in the optical potentials than are the extracted values of U_1 .

IV. DISCUSSION AND CONCLUSIONS

A. $^{27}\text{Al}(^3\text{He}, ^3\text{He}')^{27}\text{Al}$ Reaction

The five levels excited in the $(^3\text{He}, ^3\text{He}')$ reaction were assumed to be the five members of the multiplet of levels resulting from the weak coupling of

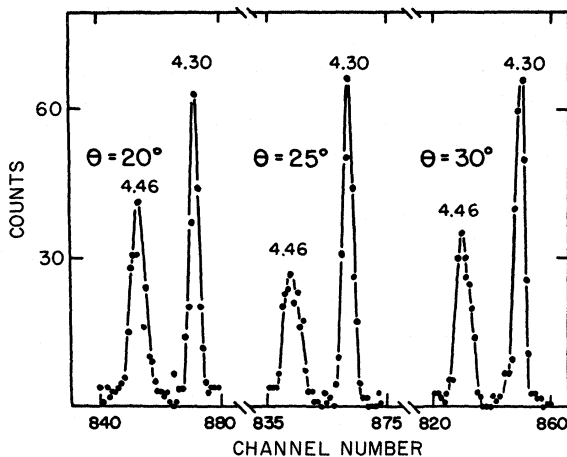


FIG. 2. Detail of $^{27}\text{Al}(^3\text{He}, t)^{27}\text{Si}$ spectra showing the 4.46-MeV doublet, together with the 4.30-MeV level.

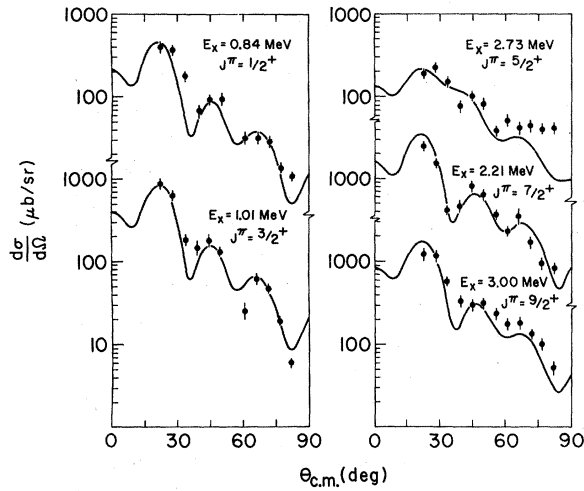


FIG. 3. Angular distributions of inelastically scattered particles leading to the low-lying states of ^{27}Al . Also shown are DWBA fits as discussed in the text.

a $1d_{5/2}$ proton hole to the $J^\pi = 2^+$ collective state at 1.78 MeV excitation in ^{28}Si . This model has been reasonably successful in interpreting (p, p') ,¹⁵ (d, d') ,¹⁶ and previous $(^3\text{He}, ^3\text{He}')$ ¹⁷ inelastic scattering reactions on ^{27}Al . It is well known that this structural model fails to predict many of the electromagnetic properties of these states; the model was chosen here primarily because it provided a simple consistent means of comparing the inelastic and charge-exchange reactions. Since ^{27}Al and ^{27}Si are known to be good mirrors, differences in the reaction processes due to structural effects alone are not expected.

The results for the collective-model DWBA calculations for the inelastic scattering are shown in Fig. 3 and Table III. The β_2 values for the $\frac{1}{2}^+$, $\frac{3}{2}^+$, and $\frac{9}{2}^+$ levels are seen to be very similar, and in addition are similar to that of ^{28}Si .¹⁸ The small value of β_2 for the 2.73-MeV level is in good agreement with that of other inelastic scattering studies.^{15, 16} This small value has been attributed¹⁵

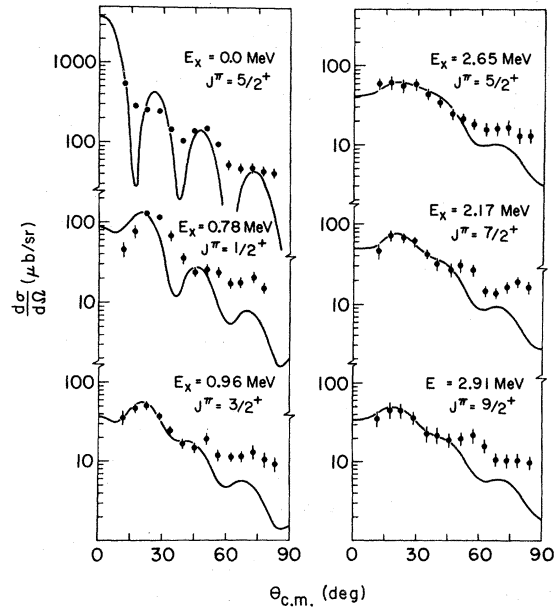


FIG. 4. Angular distributions of tritons from the ^{27}Al - $(^3\text{He}, t)^{27}\text{Si}$ reaction leading to low-lying states of ^{27}Si , along with DWBA fits.

to mixture into this state of the ^{27}Al "ground-state" structure, that is, a $1d_{5/2}$ proton hole coupled to the ground state of ^{28}Si . Crawley and Garvey¹⁵ discovered that this mixture explained the proton inelastic scattering cross sections leading to these levels using an essentially constant value of β_2 . This mixture also provides a possible explanation of the poor quality of the $L=2$ fit for the 2.73-MeV level. With mixing, $L=0$ and 4 transfer are permitted; an $L=4$ mixture is seen in Fig. 3 to improve the fit to this level considerably. The large value of β_2 for the $\frac{7}{2}^+$ 2.21-MeV level is not consistent with previous investigations, and has no simple explanation within the framework of the weak-coupling structural model. It is interesting to point out in this connection that if the low-lying states of ^{27}Al are described in terms of a ground-state rotational band, the transition to the $\frac{7}{2}^+$ level is favored by angular momentum coupling factors.

TABLE II. Description of radial form factors for all calculations.

| Final states | Radial shape | Real interaction | | | Imaginary interaction | | |
|---------------------------------|----------------------------|------------------|---------------|-------|-----------------------|---------------|-------|
| | | U (MeV) | r_v (fm) | a_v | U (MeV) | r_w (fm) | a_w |
| ^{27}Al excited states | 1st derivative Woods-Saxon | 177 | 1.14 | 0.724 | | (None used) | |
| ^{27}Si ground state | 1st derivative Woods-Saxon | 164 | 1.14 | 0.724 | 164 | 1.602 | 0.74 |
| ^{27}Si excited states | 2nd derivative Woods-Saxon | 164 | 1.14 | 0.724 | 164 | 1.602 | 0.74 |

TABLE III. Results of the collective-model calculations for the $^{27}\text{Al}(^3\text{He}, ^3\text{He}')^{27}\text{Al}$ reaction.

| E_x (MeV) | J^π | U_0 (MeV) | $\frac{(2J+1)\beta_2^2}{30}$ | $ \beta_2 $ |
|----------------|-----------------|----------------|------------------------------|-------------|
| 0.84 | $\frac{1}{2}^+$ | 177 | 0.87×10^{-2} | 0.36 |
| 1.01 | $\frac{3}{2}^+$ | 177 | 1.86×10^{-2} | 0.37 |
| 2.21 | $\frac{7}{2}^+$ | 177 | 8.36×10^{-2} | 0.56 |
| 2.73 | $\frac{5}{2}^+$ | 177 | 0.64×10^{-2} | 0.18 |
| 3.00 | $\frac{9}{2}^+$ | 177 | 4.31×10^{-2} | 0.36 |

B. $^{27}\text{Al}(^3\text{He}, t)^{27}\text{Si}$ Reaction

The low-lying states of ^{27}Si , by analogy with the mirror nucleus ^{27}Al , were assumed to consist mainly of a $1d_{5/2}$ neutron hole weakly coupled to the 2^+ collective level at 1.78 MeV in ^{28}Si . The corresponding DWBA calculations were performed, using the second term in Eq. (5) as the effective interaction. Again the deformation β was treated as a parameter; the interaction strength U_1 was derived from the ground-state analog transition. The analog-transition calculation was performed using a complex surface-peaked interaction with the geometric parameters of the real and imaginary parts equal to those of the entrance-channel optical potential. The strengths of the real and imaginary parts were taken to be identical. The fit shown in Fig. 4 corresponds to $U_1 = 164$ MeV. This value was used in all the subsequent $L=2$ and 4 calculations for the excited levels.

Pure $L=2$ calculations were seen to give a poor fit to the excited-state data. The strong maximum near 25° is predicted by the calculations, but the experimental maximum is in general broader than the theoretical one. In addition, the theoretical cross sections diminish at backward angles con-

TABLE IV. Results of the collective-model calculations for the $^{27}\text{Al}(^3\text{He}, t)^{27}\text{Si}$ reaction.

| E_x (MeV) | J^π | U_1 (MeV) | $ \beta_2 ^a$ | $ \beta_2' ^b$ | $ \beta_4' ^b$ |
|----------------|-----------------|----------------|---------------|----------------|----------------|
| 0.78 | $\frac{1}{2}^+$ | 164 | 1.62 | 1.62 | ... |
| 0.96 | $\frac{3}{2}^+$ | 164 | 0.84 | 0.79 | 0.83 |
| 2.17 | $\frac{7}{2}^+$ | 164 | 0.75 | 0.65 | 0.94 |
| 2.65 | $\frac{5}{2}^+$ | 164 | 0.59 | 0.43 | 1.32 |
| 2.91 | $\frac{9}{2}^+$ | 164 | 0.80 | 0.69 | 0.69 |

^a Calculated from best pure $L=2$ fit.

^b Calculated from best mixture of $L=2$ and 4 predictions.

siderably faster than do the experimental ones. An exception to both of these observations is the $J^\pi = \frac{1}{2}^+$ state at 0.78 MeV. In that case the poor-ness of the fit seems to be due to a uniform angular shift of the predicted angular distribution; if the calculated distribution is shifted uniformly 5° towards larger angles, the width of the maximum and the rate of diminishing are both well reproduced. The same angular shift can be seen for the $(^3\text{He}, ^3\text{He}')$ data to the $J^\pi = \frac{1}{2}^+$ level at 0.84 MeV in ^{27}Al , shown in Fig. 3, although the shift is somewhat smaller in that case. Thus, although the pure $L=2$ calculation fails to fit any of the low-lying levels, there seems to be a distinction between the $J^\pi = \frac{1}{2}^+$ level and the remainder of the levels.

Incoherent mixtures of collective-model DWBA predictions for $L=4$ were found to improve the fits to the data considerably in all cases. It is important to note that this hexadecapole transition strength cannot be explained by the first-order macroscopic DWBA. The possibility of large percentage of these states in the $J^\pi = 4^+$ collective state at 4.61 MeV in ^{28}Si is ruled out by the weakness of the $L=4$ component in the inelastic scattering transitions to the corresponding mirror levels. The final analysis of these excited-state data was thus carried out without attempting to remain consistent with the simple model employed for the inelastic scattering. The quantities β_2 and β_4 derived from the analysis are simply parameters which indicate the relative importance of the parts of the total transition amplitude which have quad-

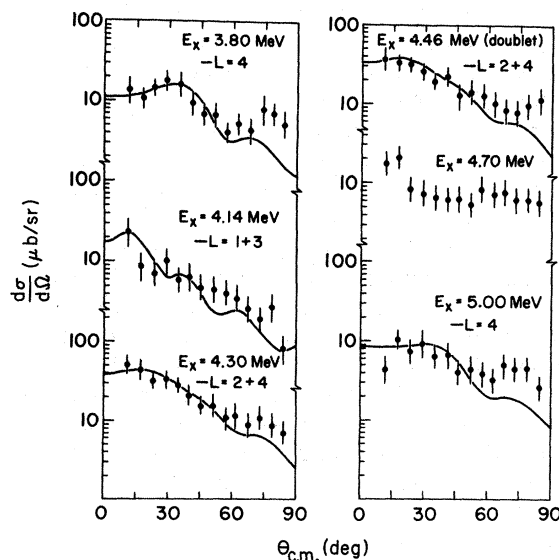


FIG. 5. Angular distributions of tritons leading to states in ^{27}Si above 2.91 MeV excitation. Also shown are DWBA fits.

ruple and hexadecapole transformation properties. Figure 4 and Table IV show the results of the final calculations.

C. Higher-Lying Levels

The $^{27}\text{Al}(^3\text{He}, ^3\text{He}')^{27}\text{Al}$ reaction populated the levels above 3.00 MeV excitation only very weakly relative to the low-lying states. However, the inelastic scattering cross sections to the low-lying states are considerably larger than those for the $(^3\text{He}, t)$ reaction to the mirror states. Inelastic cross sections whose magnitudes are comparable to the $(^3\text{He}, t)$ cross sections could easily be obscured by the continuum resulting from slit-scattered elastic particles. In the $^{27}\text{Al}(^3\text{He}, t)^{27}\text{Si}$ reaction, however, angular distributions were extracted for six levels ranging from 3.80 to 5.00 MeV excitation. The six angular distributions obtained are shown in Fig. 5. A previously known level at 3.54 MeV excitation¹⁹ was populated too weakly for the extraction of an angular distribution.

The level at 3.80 MeV is known to have spin $\frac{3}{2}$, with the parity unknown.²⁰ The electromagnetic properties of this and nearby levels²⁰ suggest that it is the mirror of the 3.96-MeV level in ^{27}Al , which has spin and parity $J^\pi = \frac{3}{2}^+$.¹⁹ It is therefore interesting to note that the shape of the angular distribution for this state is best fitted with an $L=4$ DWBA curve as can be seen in Fig. 5. This result is similar to a previously reported case in ^{23}Mg , where a $\frac{3}{2}^+$ to $\frac{7}{2}^+$ $(^3\text{He}, t)$ transition was discovered to be dominated by $L=4$ transfer.²¹

With the assumption of a direct reaction mechanism, the forward data points for the 4.14-MeV level are characteristic of low angular momentum transfer. Comparison of the γ decay of this level with that of the 4.05-MeV level in ^{27}Al strongly suggests that these are mirror states, with $J^\pi = \frac{1}{2}^-$ ($\frac{3}{2}^-$).²⁰ The solid line in Fig. 5 is an incoherent mixture of collective-model DWBA calculations for $L=1$ and 3.

Angular-correlation studies for this laboratory have assigned spin $\frac{5}{2}$ to the 4.30-MeV level, and have suggested positive parity on the basis of the strong similarity of the decay scheme of this level to that of the 4.41-MeV level in ^{27}Al .²² The solid line in Fig. 5 is the result of collective-model DWBA calculations assuming an incoherent mixture of $L=2$ and 4. The mixture yielding the best fit corresponds to considerable $L=4$ admixture.

The angular distribution of the unresolved doublet near 4.46 MeV is shown in Fig. 5. It has been suggested^{11, 22} that these levels are the analogs of the 4.51- and 4.58-MeV levels of ^{27}Al . The solid curve in Fig. 5 is an incoherent mixture of col-

lective-model DWBA predictions for $L=2$ and 4. The large $L=4$ component can conceivably correspond to the excitation of the $J^\pi = \frac{11}{2}^+$ analog of the ^{27}Al 4.51-MeV level.

The angular distribution for the 4.70-MeV level is very unusual and could not be fitted with any DWBA predictions. The level at 5.00 MeV excitation was populated very weakly. The general trend of the data seems to correspond to high angular momentum transfer. The solid curve in Fig. 5 is the result of a collective-model DWBA calculation for $L=4$.

D. Conclusions

The inelastic scattering of ^3He from ^{27}Al at 18-MeV incident energy is reasonably well described by the collective-model DWBA. In agreement with (p, p') , (d, d') , and previous $(^3\text{He}, ^3\text{He}')$ investigations, the relative populations of the low-lying states are well reproduced by the assumption of weak coupling. The selectivity of final states excited by the $(^3\text{He}, ^3\text{He}')$ reaction also is consistent with this structural picture. The weak-coupling picture, although considered in general to be inadequate, still provides a convenient formalism for reduction of the inelastic scattering data to a few simple parameters which then provide easy comparison with the charge-exchange reaction leading to the mirror nucleus.

The over-all quality of the fits, including a mild Q -value dependence of the angular-distribution shape, indicates that the assumption of pure $L=2$ transfer is quite good, except in the case of the $J^\pi = \frac{5}{2}^+$ level at 2.73 MeV. The β_2 values yielded by the calculation are very close to the known value of β_2 for ^{28}Si ¹⁸; their large magnitudes, according to the criterion of Bassel *et al.*,⁶ indicate that greater accuracy could probably be obtained using the coupled-channels formalism.

The analog transition to the ^{27}Si ground state was quite well reproduced by the collective-model DWBA using the symmetry potential as described in Sec. III B. The strength of the interaction potential U_1 was determined to be 164 MeV. This is consistent with the trend suggested in Ref. 9 that U_1 increases with decreasing bombarding energy. However, caution should be used in drawing any conclusion from the absolute value of U_1 because it does depend sensitively on the geometry of the form factor used.

The $(^3\text{He}, t)$ transitions to excited levels in ^{27}Si were observed to be dissimilar from the inelastic scattering in three primary respects. First, the $(^3\text{He}, t)$ cross sections to low-lying states are only about 6–10% of the inelastic cross sections to the mirror states. This result is qualitatively under-

stood in the macroscopic model; the symmetry term in the optical potential is considerably smaller than the real potential. Second, the $(^3\text{He}, t)$ reactions imply a quadrupole deformation which is about twice as large as that yielded by the inelastic scattering or by electromagnetic measurements. This large value is in agreement with previous observations⁴; various explanations have been proposed and have been discussed in the Introduction. Finally, the reactions were observed to be dissimilar in that the angular-distribution shapes for the $(^3\text{He}, t)$ transitions to low-lying states were not well fitted by pure $L=2$ calculations; mixture of $L=4$ contributions improved the fits considerably for the excited states. These $L=4$ contributions have not been observed in previous investigations; they have no simple explanation in the single-step macroscopic DWBA interpretation of these transitions. It is important to

note that the calculations in which $L=2$ and 4 are considered are not based on a structural model: The quantities β_4 are simply parameters expressing the strengths of the $L=4$ contributions. Thus, it is not surprising that the values of β_4 obtained in the present study are very large relative to the hexadecapole deformations recently measured for ^{28}Si using the inelastic scattering of 104-MeV α particles.¹⁸ Perhaps the most reasonable explanation for the $L=4$ contributions to the angular distributions lies in the microscopic configurations of the states. Certainly, charge exchange on a $d_{5/2}$ nucleon can give $L=4$ contributions. Such $L=4$ terms would, of course, also be present in a microscopic description of the inelastic scattering process. However, since the collective inelastic cross section is larger by a factor of 10–20, such contributions could easily go undetected in the inelastic scattering.

*Work supported by the National Science Foundation.

†Present address: Department of Physics, University of Pittsburgh, Pittsburgh, Penna. 15213.

¹E. H. Schwarcz, *Phys. Rev.* **149**, 752 (1966).

²V. A. Madsen, *Nucl. Phys.* **80**, 177 (1966).

³J. J. Wesolowski, E. H. Schwarcz, P. G. Roos, and C. A. Ludemann, *Phys. Rev.* **169**, 878 (1968).

⁴P. D. Kunz, E. Rost, R. R. Johnson, G. D. Jones, and S. I. Hayakawa, *Phys. Rev.* **185**, 1528 (1969).

⁵W. E. Frahn and G. Weichers, *Phys. Letters* **26B**, 5 (1967); W. E. Frahn, *Nucl. Phys.* **A107**, 129 (1968); W. E. Frahn and G. Weichers, *Nucl. Phys.* **A113**, 593 (1968).

⁶R. H. Bassel, G. R. Satchler, R. M. Drisko, and E. Rost, *Phys. Rev.* **128**, 2693 (1962).

⁷T. Tamura, *Rev. Mod. Phys.* **37**, 679 (1965).

⁸G. R. Satchler, in *Isospin in Nuclear Physics*, edited by D. H. Wilkinson (American Elsevier, New York, 1969), Chap. 9.

⁹W. L. Fadner, J. J. Kraushaar, and S. I. Hayakawa, *Phys. Rev. C* **5**, 859 (1972).

¹⁰F. S. Goulding, D. A. Landis, J. J. Cerny, and R. H. Pehl, *Nucl. Instr. Methods* **31**, 1 (1964).

¹¹F. C. Barker, K. W. Carter, D. C. Kean, C. J. Piluso, and R. H. Spear, *Australian J. Phys.* **24**, 1 (1971).

¹²G. R. Satchler, *Phys. Letters* **39B**, 492 (1972) and references therein.

¹³Distorted-wave code of P. D. Kunz, University of Colorado (unpublished).

¹⁴J. E. Holden, D. P. Balamuth, H. T. Fortune, and R. W. Zurmühle, *Bull. Am. Phys. Soc.* **15**, 544 (1970).

¹⁵G. M. Crawley and G. T. Garvey, *Phys. Rev.* **167**, 1070 (1968).

¹⁶H. Niewodniczanski, J. Nurzynski, A. Stralkowski, J. Wilczynski, J. R. Rook, and P. E. Hodgson, *Nucl. Phys.* **55**, 386 (1964).

¹⁷K. P. Artemov, V. Z. Goldberg, and V. P. Rudakov, *Yadern. Fiz.* **9**, 266 (1969) [transl.: *Soviet J. Nucl. Phys.* **9**, 157 (1969)].

¹⁸H. Rebel, G. W. Schweimer, G. Schatz, J. Specht, R. Löhken, G. Hauser, D. Habs, and H. Klewe-Nebenius, *Nucl. Phys.* **A182**, 145 (1972), and references therein.

¹⁹P. M. Endt and C. Van der Leun, *Nucl. Phys.* **A105**, 1 (1967).

²⁰M. B. Lewis, N. R. Roberson, and D. R. Tilley, *Phys. Rev.* **137**, B1464 (1965).

²¹J. E. Holden, H. T. Fortune, D. P. Balamuth, and R. W. Zurmühle, *Phys. Rev. Letters* **25**, 1677 (1970).

²²D. P. Balamuth, J. E. Holden, and R. W. Zurmühle, *Phys. Rev. C* **5**, 476 (1972).